Available online at www.sciencedirect.com
ScienceDirect
Ceramics International 37 (2011) 2513–2518
CERAMICS INTERNATIONAL
www.elsevier.com/locate/ceramint

Structural investigation of mechanically activated nanocrystalline $BaTiO_3$ powders

V.P. Pavlović [a,*], J. Krstić [b], M.J. Šćepanović [c], J. Dojčilović [d], D.M. Minić [e], J. Blanuša [f], S. Stevanović [g], V. Mitić [g], V.B. Pavlović [h]

[a] Faculty of Mechanical Engineering, University of Belgrade, Kraljice Marije 16, Belgrade, Serbia
[b] Institute of Chemistry, Technology and Metallurgy, Department of Catalysis and Chemical Engineering, Belgrade, Serbia
[c] Center for Solid State Physics and New Materials, Institute of Physics, Belgrade, Serbia
[d] Faculty of Physics, University of Belgrade, Belgrade, Serbia
[e] Faculty of Physical Chemistry, University of Belgrade, Belgrade, Serbia
[f] Vinca Institute of Nuclear Sciences, Belgrade, Serbia
[g] Institute of Technical Sciences of the SASA, Belgrade, Serbia
[h] Joint Laboratory for Advanced Materials of the Serbian Academy of Sciences and Arts, Belgrade, Serbia

Received 11 February 2011; received in revised form 25 March 2011; accepted 31 March 2011
Available online 9 April 2011

Abstract

In this article, in order to obtain tetragonal nanocrystalline $BaTiO_3$, structural investigations of mechanically activated $BaTiO_3$ powder have been performed. A mercury porosimetry analysis and scanning electron microscopy method have been applied for determination of the specific pore volume, porosity and microstructure morphology of the samples. The lattice vibration spectra of nonactivated and activated powders, their phase composition, lattice microstrains and the mean size of coherently diffracting domains were examined by Raman spectroscopy and the X-ray powder diffraction method. The average crystal structure of obtained nanocrystalline powders, estimated from X-ray diffraction data, gave evidence of retained, but slightly sustained tetragonality of powders, even for particles as small as ~30 nm. Raman spectroscopy also gave clear evidence for local tetragonal symmetries, in particular through the presence of a band at ~307 cm^{-1}.

Keywords: Nanocrystalline $BaTiO_3$; Mechanical activation; X-ray diffraction; Raman spectroscopy

1. Introduction

It is well known that advances in microelectronics and communication industries have led to substantial miniaturization of many electronic devices such as multilayer ceramic capacitors (MLCC), while the performance requirements have increased [1]. During MLCC production process, a mixture of ceramic powder and binder solution is formed into green ceramic sheets by tape casting. Therefore, miniaturization requires smaller and more uniform powder particle sizes of many electroceramic materials [2]. For $BaTiO_3$ ceramics, which can be applied not only in ceramic capacitors, but also in self-controlled heaters, communication filters and nonvolatile memories, a narrow powder particle size distribution and high tetragonality is required. Unfortunately, most methods for the production of $BaTiO_3$ fine powders, such as the conventional solid state reaction method, alkoxide-hydroxide route, solvothermal process, hydrothermal methods, etc., are unsuccessful in preparing $BaTiO_3$ nanopowder with a tetragonal phase. It has been established that, depending on the processing route which has been used, size effects and the formation of lattice OH^- groups, associated with strains and defects, are factors which stabilize the metastable cubic structure in $BaTiO_3$ [3,4]. As a result, formation of tetragonal $BaTiO_3$ nanopowder is suspended. Recently, Park et al. [5] reported that nanograined $BaTiO_3$ ceramics prepared from noncoated $BaTiO_3$ nanopowders showed a mixed state of cubic and tetragonal phases. Their results indicate not only the possibility of tetragonal $BaTiO_3$ nanopowder formation, but also emphasize that developing of a low temperature synthesis procedure directly resulting in the

* Corresponding author.
E-mail address: vppavlovic@sbb.rs (V.P. Pavlović).

0272-8842/$36.00
doi:10.1016/j.ceramint.2011.03.064

formation of tetragonal $BaTiO_3$ nanopowders is of extreme interest.

In order to produce nanocrystalline powders and improve the final properties of electroceramics, in recent years, among the other methods, high energy mechanical activation has been employed [6]. Several investigations have been carried out in order to obtain $BaTiO_3$ by mechanically activating the reactants [7,8]. $BaTiO_3$ resulted from milling of $BaO + TiO_2$ in a ball mill during 100 h [9], however high temperature treatments were needed to preserve BaO in the pure state, prior to the milling. Also, the milling in a planetary mill of $Ba(OH)_2{\cdot}8H_2O + TiO_2$ resulted in a $BaTiO_3$ powder which had poor crystallinity, so an annealing treatment was necessary [10]. Unfortunately, all these synthesis procedures failed to create $BaTiO_3$ powder with a tetragonal structure. Although production of nanocrystalline powders by mechanical activation can be done not only by mechanochemical processes, but also by activation of a single phase powder (by controlling the balance point between fracturing and cold welding) [11], no systematic investigation of single phase $BaTiO_3$ mechanical activation has been performed yet. These investigations are very important since mechanical activation of initial powder change its structure and reactivity and enable obtaining ceramics with improved final properties. Therefore, in order to investigate the possibility of obtaining tetragonal nanocrystalline $BaTiO_3$, structural investigations of mechanically activated $BaTiO_3$ powder have been presented in this article.

2. Experimental procedure

As the starting material, a high purity commercial $BaTiO_3$ powder (Aldrich, 99.9% purity, mean grain size < 2 μm) was used. Mechanical activation was carried out in a planetary-ball mill (Fritsch Pulverissete 5) for 10, 20, 40 and 60 min in an agate jar with 8 mm in diameter agate balls. The ball/sample mass ratio was 20:1 while the tray and vial rotation speeds were 317 and 396 rpm, respectively.

The influence of mechanical activation on the change of the specimen's bulk density, specific pore volume and total porosity, have been performed using the mercury porosimetry analysis. Bulk density (ρ_{bl}) and specific pore volume (V_{sp}) of all samples were estimated with a Carlo Erba Porosimeter 2000 using the Milestone 100 Software System. This type of high-pressure mercury intrusion porosimeter operates up to 207 MPa, enabling determination of the total pore volume of all pores greater than 7.5 nm in diameter. The total porosity of the sample (P) was determined as a product of V_{sp} and ρ_{bl}.

The microstructure morphology of nonactivated and activated samples has been investigated using scanning electron microscopy (JEOL-JSM-T20).

X-ray powder diffraction patterns of the initial and activated powders were obtained in Bragg-Brentano geometry, on a Philips PW-1010 powder diffractometer, using Ni-filtered Cu K_α radiation. The diffracted intensities were collected in a step scan mode 0.02°/12 s, over the 2θ angular range 10–120°. Structural refinements were carried out using the Rietveld method and the Koalariet-Xfit computer program with algorithms described by Coelho and Cheary [12].

Room temperature Raman spectra of the initial and activated samples were obtained in the spectral range from 200 to 1000 cm^{-1}, in the backscattering geometry, by a Micro Raman Chromex 2000, using the 532 nm line of a Nd:YAG laser. The spectral resolution was 1 cm^{-1}. The laser output power was 50 mW and the laser beam was focused to a spot size of 5 μm at the sample surface.

3. Results and discussion

In general, during mechanical activation the introduction of mechanical energy may cause numerous processes such as a refinement in crystallite size, creation and movement of structural defects, activation of phonons, amorphisation of the crystalline phase, phase transformations, order–disorder transitions and chemical reactions [13]. Although during the formation of mechanically activated nanocrystalline powders, in a size reduction process, powder particles break in dependence on the applied stress and material properties, the production of nanoparticles does not only depend on particle comminution, but also on the capability of stabilization of broken fragments and their rheology [14]. When powder particles are subjected to a mechanical stress which exceeds their strength, the formation of cracks is initiated. As the cracks propagate, the stored strain energy releases, leading eventually to particle fracture. In the case when the strength of the material is exceeded locally, especially for particles of irregular shape, the erosion of the particle surface, accompanied with the rise of the strain and defect concentration, may occur [15]. As a result, the change of the powder particle morphology and powder porosity (which is manifested by interparticle voids and pores within individual particles) emerges. Those changes can be analyzed by measuring specific pore volume, bulk density, specific surface area and total porosity.

Our investigations showed that mechanical activation caused a significant decrease of specific pore volume (V_{sp}) and total porosity (P) for the activation time up to 20 min, especially for the first 10 min (Fig. 1a and b). Further increase of the activation time has not led to a significant change of V_{sp} and P. On the other hand, the maximum values of bulk density (ρ_{bl}) were obtained for activation up to 10 min, after which the decrease of ρ_{bl} has been noticed. However, the bulk density values of the activated samples still remained significantly above the value of the nonactivated one, even for the longest time of activation. Considering the change in porosity, it is clear that a pore system reduction, which is caused by the fraction of particles during activation and expressed through the drop of V_{sp}, is a dominant phenomena for the activation up to 10 min. Namely, the calculated value of relative decrease of V_{sp} during the first 10 min of the activation was ~35.4%, while the relative increase of ρ_{bl} was just ~14.6%. Therefore, the total porosity of the samples significantly decreased in comparison with the nonactivated material. Mechanical activation also caused the change of the specific surface from 2.42 m^2/g for the

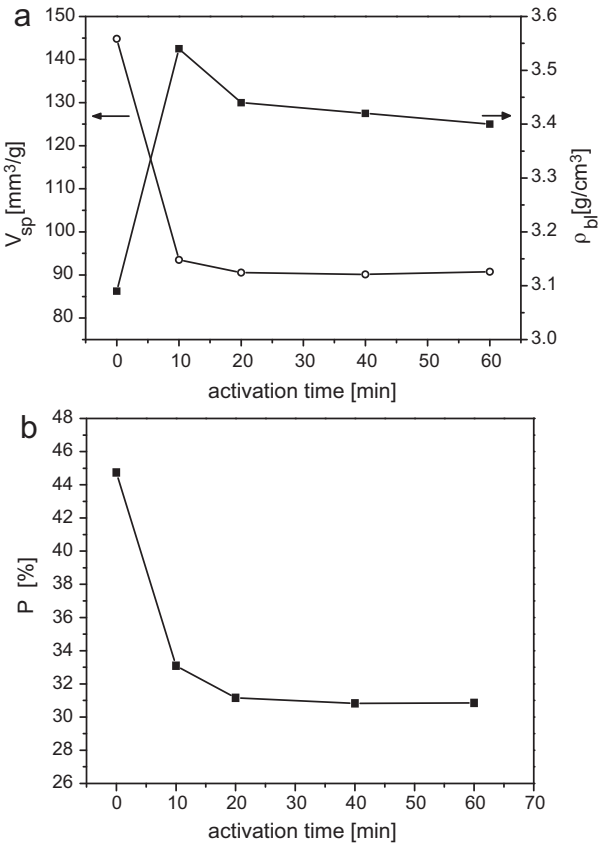

Fig. 1. (a) Specific volume and bulk densities of mechanically activated $BaTiO_3$. (b) Total porosity of mechanically activated $BaTiO_3$.

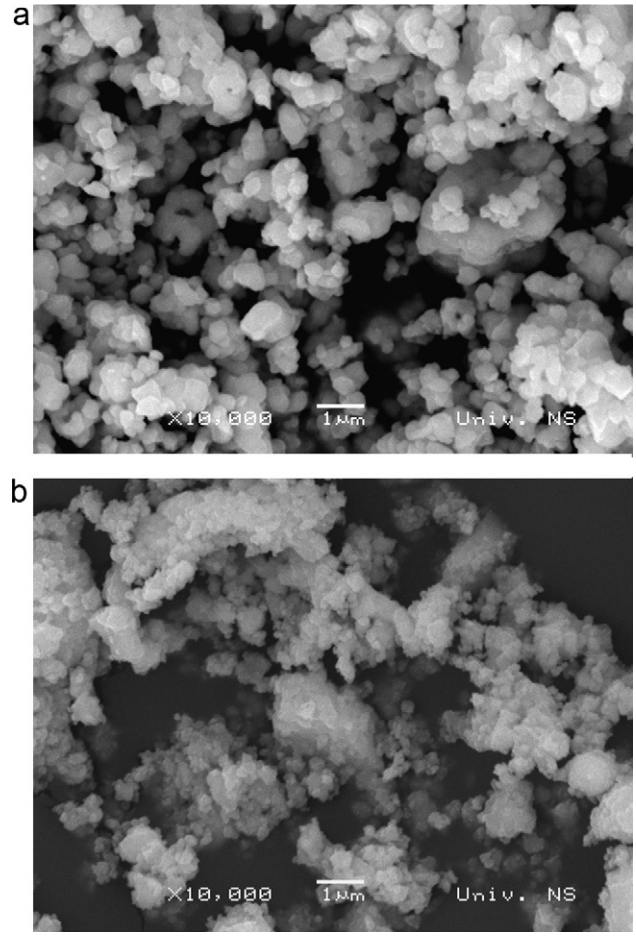

Fig. 2. (a) Microstructure of nonactivated $BaTiO_3$. (b) Microstructure of $BaTiO_3$ activated for 40 min.

nonactivated samples, up to 4.49, 4.07, 4.06 and 4.02 for the samples activated for 10, 20, 40 and 60 min. The change of the specific surface and a decrease of the bulk densities of the samples activated for more than 10 min can be attributed to powder particle aglomeration, which is a consequence of an increase of the particle surface energy during comminution of the initial powder particles. It should be noticed that the tendency of agglomeration, considerably influences the sintering and final properties of $BaTiO_3$ ceramics. According to our previous investigations [16] a densification rate curve for mechanically activated $BaTiO_3$ samples can be divided into three process. The first process is attributed to intra-agglomerate particle sintering, the second one to sintering of grains between agglomerates, while the third one can be attributed to agglomerate sintering. As a result, mechanical activation change the microstructure of sintered material and significantly affects final electrical properties of $BaTiO_3$ ceramics [17].

The results obtained from mercury porosimetry analysis are in accordance with the results obtained by SEM (Fig. 2). According to them, mechanical activation has led to the formation of new surfaces and comminution of the initial powder particles. It should be noticed that during the formation of new surfaces, excess of the energy in the surface occurs, which together with particle diminution may influence the producing and properties of the nanocrystalline material [18].

Our X-ray analysis indicated that mechanical activation, in spite of powder particle diminution, did not change the tetragonal structure of the initial powder into the cubic one (Fig. 3) [JCPDS Card No. 5-626]. The increase in structural disorder during activation resulted only in a decrease of the integral intensity of XRD reflections and broadening of diffraction profiles (Fig. 4). This can be attributed to destabilization of the crystalline phase, refinement in particle and crystallite sizes and generation of stress fields. It should be noticed that destabilization of the crystalline phase is thought to occur by the accumulation of structural defects such as vacancies, dislocations, grain boundaries and it may lead to the formation of amorphous domains for increased activation time. Although the mechanism of amorphization by mechanical activation is not clearly understood, it seems to follow the sequence [19]: ordered phase → disordered phase → fine-grained (nanocrystalline) phase → amorphous phase.

Since significant peak broadening, which is characteristic for the formation of amorphous domains, did not occurred in our diffraction patterns, we have concluded that in our case the activation time required for amorphization has not been reached, that is mechanical activation of $BaTiO_3$ powder up to 60 min resulted only in the formation of a nanocrystalline $BaTiO_3$ phase. In order to obtain the crystallite size and

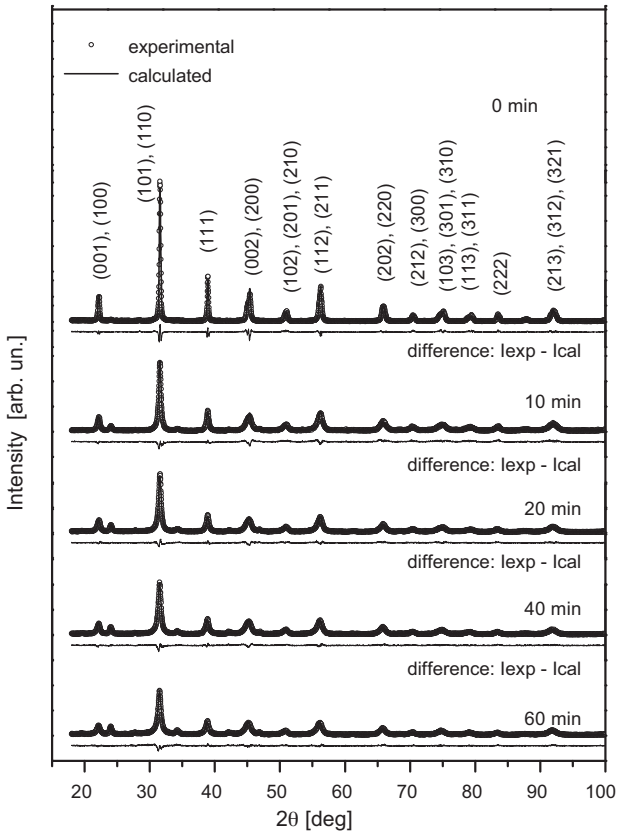

Fig. 3. The structural refinement patterns of nonactivated and activated $BaTiO_3$ using X-ray powder diffraction data based on the tetragonal phase.

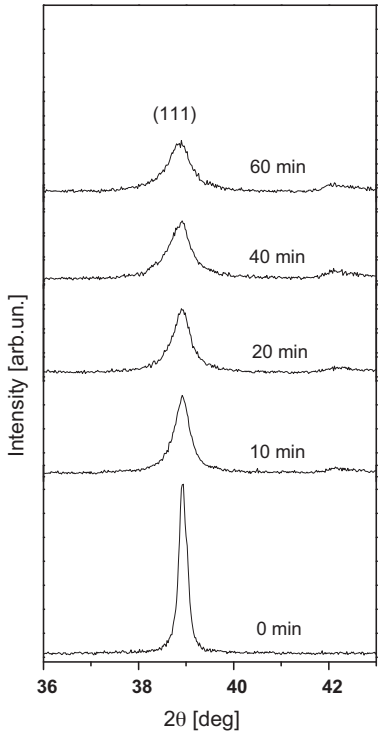

Fig. 4. Broadening of XRD profile of (1 1 1) reflection in nonactivated and activated $BaTiO_3$.

microstrain of the nonactivated and activated samples, the Rietveld method has been applied. This method is based on the whole profile fitting methodology and all reflections can be analyzed with sufficient accuracy [17]. During the analysis, the process of successive profile refinement was applied, until convergence was reached [20]. Obtained values of *Rwp* (weighted residual factor) varied from 9.8% (for the nonactivated samples) to 12.6% (for samples activated for 60 min). The refinement showed that as a result of mechanical activation tetragonal nanocrystalline $BaTiO_3$ is formed. It was observed that mechanical activation led to a significant decrease of the mean crystallite size from 150 nm for the nonactivated samples, down to 45 nm, 39 nm, 34.5 nm and 30.5 nm, for samples activated for 10, 20, 40 and 60 min, respectively. At the same time, the generation of stress fields at the particle edge caused increase of the sample microstrains from 0.1 for the nonactivated samples up to 0.47, 0.61, 0.7 and 0.74 for the samples activated for 10, 20, 40 and 60 min.

According to our previous investigations, the formation of uncompensated stress during mechanical activation can influence the tetragonal distortion, thus leading to modification of the phase transition temperature and electrical properties of the sintered material [19]. Furthermore, numerous authors have established that with decreasing of the crystallite size the tetragonal distortion of the unit cell of $BaTiO_3$, which is a precondition for the presence of ferroelectricity, alters over the pseudocubic to cubic, and finally disappears below a certain critical size value [21–28]. The possible responsible mechanism for this phenomenon is still under controversial discussion. Arlt et al. proposed that a pseudocubic, paraelectric modification of $BaTiO_3$ is stabilized through internal stresses, which arise from mechanical constraints at the boundaries, while Frey et al. [22] suggested the so-called ''brick wall model'', assuming that the ceramic grains consist of a tetragonal ferroelectric core, which is surrounded by a thin layer of a cubic phase, with a substantially lower dielectric constant. It is important to notice that the critical crystallite value, which enables stabilization of the room temperature cubic structure, depends on the powder preparation method and usually ranges from 20 to 100 nm [23–26]. Our investigations showed that the applied mechanical activation can lead to the formation of nanocrystalline $BaTiO_3$ powder with a tetragonal structure, even for particles as small as ∼30 nm. Since the formation of micrometer powder particles with a tetragonal structure, as well as cubic nanocrystalline powder particles, are not convenient for application in multilayer ceramic capacitors production, direct generation of nanocrystalline, tetragonal $BaTiO_3$ is of considerable interest [29].

The results of the X-ray analysis are in accordance with those obtained by Raman spectroscopy measurements. Raman spectroscopy has been employed to determine the lattice vibrational spectra of nc-$BaTiO_3$ powders. It is well known that symmetry-group analysis in cubic $BaTiO_3$ predicts no Raman active modes, while in tetragonal $BaTiO_3$ (space group *P*4*mm*) it predicts eight optical Raman active modes: 4 modes of E symmetry, 3 modes of A_1 symmetry and one mode of B_1 symmetry [1,24,30–33]. Each of these modes splits into

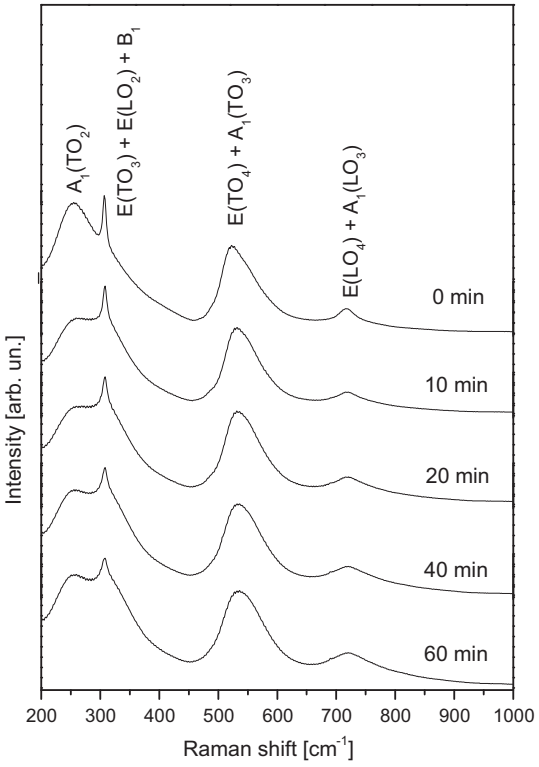

Fig. 5. Micro-Raman spectra of nonactivated and activated $BaTiO_3$.

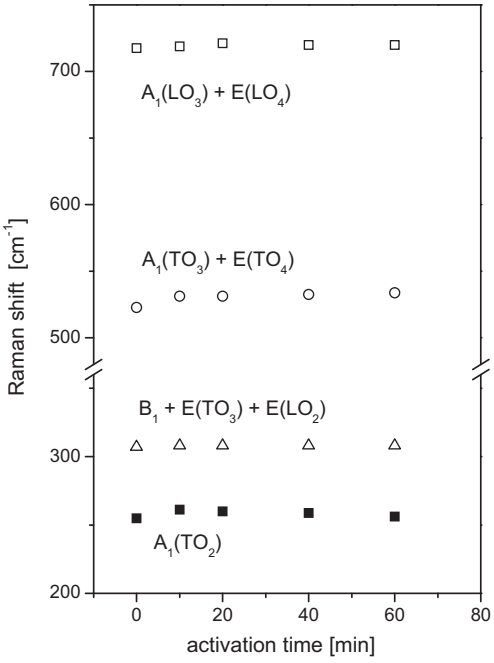

Fig. 6. Activation time dependence of the Raman band positions of $BaTiO_3$ samples.

transverse (TO) and longitudinal (LO) optical components, due to long-range electrostatic forces associated with lattice ionicity [24,30,32]. The number of Raman peaks in experimentally obtained unpolarized spectrum of polycrystalline samples is commonly less than the number of theoretically derived modes, not only because of great overlapping of A_1 and E modes, as well as B_1 and E modes, which frequencies are very close to one another, but also due to the existence of a coupled-mode interaction and overdamped character of the lowest optical E mode ($E(TO_1)$ soft mode).

In our investigations, four Raman peaks have been recorded and assigned to more than one phonon mode of tetragonal $BaTiO_3$, as presented in Fig. 5. According to literature data [30,34] Raman peaks were interpreted as follows: the broad peak centered around 270 cm^{-1} as a $A_1(TO_2)$ mode, a sharp peak at ~307 cm^{-1} as $B_1 + E(LO_2) + E(TO_3)$, an asymmetric broad peak at ~520 cm^{-1} as $A_1(TO_3) + E(TO_4)$ and a broad weak peak at ~720 cm^{-1} as a sum of $A_1(LO_3)$ and $E(LO_4)$ modes. The observed spectrum of the nonactivated sample agrees well with the powder Raman spectrum reported by Hoshina et al. [26], Cho et al. [32] and Naik et al. [35], as well as with those reported for some polycrystalline $BaTiO_3$ samples [30] and microcrystalline ceramics [36,37].

Our measurements show that as the applied activation time increases, the Raman modes become broader and gradually lose their intensity (Fig. 5). Such behavior of optical phonon modes is a consequence of a decrease in the observed particle and crystallite size, but also indicates a rise of lattice deformation, defect number and disorder in the longer mechanically activated powders. The estimated values of Raman-peak positions are displayed as a function of the activation time, in Fig. 6. As it can be seen, activation induced a shift to upper frequency for Raman peaks around 260 cm^{-1} and 520 cm^{-1}, particularly in comparison with the nonactivated sample. These results are in good agreement with investigations which pointed out that two asymmetric broad $A_1(TO)$ modes, at ~260 cm^{-1} and 520 cm^{-1}, are sensitive to structure defects [38]. Although as-read data indicate that the Raman peak at ~720 cm^{-1} also seems to be skewed toward the high frequency side, the accuracy of this data is reduced due to the overdamped and weak profile of that peak in the activated samples. The observed blue shift of the A_1 modes can be related to the increase in tensile stress [39] introduced by mechanical activation. The peak at 307 cm^{-1}, which appears sharp in the nonactivated sample, exhibits distinct broadening (Fig. 5), but no significant frequency shift, as the activation time increases (Fig. 6). Many investigations pointed out that the peak at 307 cm^{-1} is specific for tetragonal $BaTiO_3$, since it disappears above the Curie temperature (T_c) where the structure becomes cubic [27,28,32]. On the contrary, the persistence of Raman bands around 260 cm^{-1} and 520 cm^{-1} well beyond T_c has been reported [27,31,35], although this is not expected from the symmetry group theoretical selection rules. Since the Raman peak around 720 cm^{-1} has also been reported as observed only below the phase-transition temperature [27,31,33], the broadening accompanied by a drop in the intensity of Raman peaks around 307 cm^{-1} and 720 cm^{-1} suggest that the tetragonal structure might be slightly suppressed in activated powders [32].

4. Conclusion

In this article, the results of structural investigations of $BaTiO_3$ powders obtained by mechanical activation have been

presented. It was noticed that mechanical activation caused the decrease of the specific pore volume and total porosity, especially for the first 10 min of activation. Microstructural investigations showed that such activation has led to the creation of new surfaces and comminution of the initial powder particles. As a result, the formation of nanocrystalline $BaTiO_3$ powder has been enabled. The Rietveld method has been applied to analyze X-ray diffraction patterns in order to determine the crystallite size and microstrains of the nonactivated and activated samples. The refinement pointed out that mechanical activation led to the decrease of the mean crystallites size from 150 nm down to 30.5 nm, while the microstrains increased from 2% up to 14.8%. The average crystal structure of the obtained nanocrystalline powders, estimated from X-ray diffraction data, gave evidence of a retained, but slightly suppressed tetragonality of powders, even for particles as small as ∼30 nm. Raman spectroscopy also gave clear evidence for local tetragonal symmetries, in particular through the presence of the band at $\sim 307\ cm^{-1}$. The influence of mechanical activation on lattice vibrational spectra was expressed primarily through broadening and gradual decrease of the Raman peaks intensity.

Acknowledgements

The financial support from the Ministry of Science and Technological Development of the Republic of Serbia through Project No. 172057 is acknowledged.

References

[1] S. Wada, T. Tsurumi, H. Chikamori, T. Noma, T. Suzuki, J. Cryst. Growth 229 (2001) 433–439.
[2] T. Buscaglia, V. Buscaglia, M. Viviani, J. Petzelt, M. Savinov, L. Mitoseriu, A. Testino, P. Nanni, C. Harnagea, Z. Zhao, M. Nygren, Nanotechnology 15 (2004) 1113–1117.
[3] X. Li, W.H. Shih, J. Am. Ceram. Soc. 80 (1997) 2844.
[4] D.H. Yoon, B.I. Lee, J. Ceram. Proc. Res. 3 (2002) 41.
[5] B. Park, N.H. Cho, C.D. Kim, S.K. Lee, J. Am. Ceram. Soc. 87 (2004) 510.
[6] M. Xue, D.M. Wan, J. Wang, Solid State Ionics 151 (2002) 403–412.
[7] B. Kong, J. Ma, H. Huang, R.F. Zhang, W.X. Que, J. Alloys Compd. 337 (2002) 226–230.
[8] V.P. Pavlovic, B.D. Stojanovic, V.B. Pavlovic, Z. Marinkovic-Stanojevic, Lj. Zivkovic, M.M. Ristic, Sci. Sinter. 40 (2008) 21–26.
[9] N.J. Welham, J. Mater. Res. 13 (1998) 1607–1613.
[10] O. Abe, Y. Suzuki, Mater. Sci. Forum 225–227 (1996) 563–568.
[11] R. Janot, D. Guererd, Prog. Mater. Sci. 50 (2005) 1–92.
[12] W. Cheary, A.A. Coelho, J. Appl. Crystallogr. 25 (1992) 109–121.
[13] W. Peukert, Int. J. Miner. Process. 74S (2004) 3–17.
[14] S. Monde, F. Stenger, W. Peukert, J. Schwedes, Powder Technol. 132 (2003) 64–73.
[15] R. Hogg, A.J. Dynys, H. Cho, Powder Technol. 122 (2002) 122–128.
[16] V.P. Pavlović, M.V. Nikolić, V.B. Pavlović, N. Labus, Lj. Živković, B.D. Stojanović, Ferroelectrics 319 (2005) 75–85.
[17] V.P. Pavlovic, M.V. Nikolic, Z. Nikolic, G. Brankovic, Lj. Zivkovic, V.B. Pavlovic, M.M. Ristic, J. Eur. Ceram. Soc. 27 (2007) 575–579.
[18] B. Stojanovic, J. Mater. Process. Technol. 143–144 (2003) 78–81.
[19] C. Suryanarayana, E. Ivanov, V.V. Boldyrev, Mater. Sci. Eng. A 304–306 (2001) 151–158.
[20] S.K. Pradhan, S. Bid, M. Gateshki, Mater. Chem. Phys. 93 (2005) 224–230.
[21] G. Arlt, D. Hennings, G. deWith, J. Appl. Phys. 58 (1985) 1619–1625.
[22] M.H. Frey, Z. Xu, P. Han, D.A. Payne, Ferroelectrics 206–207 (1998) 337–353.
[23] M. Zhang, J. Yu, J. Chu, Q. Chen, W. Chen, J. Mater. Process. Technol. 137 (2003) 78–81.
[24] Y.I. Kim, J.K. Jung, K.S. Ryu, Mater. Res. Bull. 39 (2004) 1045–1053.
[25] V. Buscaglia, M. Buscaglia, M. Viviani, L. Mitoseriu, P. Nanni, V. Trefiletti, P. Piaggio, I. Gregora, T. Ostapcuh, J. Pokorny, J. Petzelt, J. Eur. Ceram. Soc. 26 (2006) 2889–2898.
[26] T. Hoshina, H. Kakemoto, T. Tsurumi, S. Wada, J. Appl. Phys. 99 (2006) 1–8, 054311.
[27] M.H. Frey, D.A. Payne, Phys. Rev. B 54 (1996) 3158–3168.
[28] K. Suzuki, K. Kijima, J. Alloys Compd. 419 (2006) 234–242.
[29] H. Xu, L. Gao, J. Am. Ceram. Soc. 86 (1) (2003) 203–205.
[30] U.D. Venkateswaran, V.M. Naik, R. Naik, Phys. Rev. B 58 (1998) 14256–14260.
[31] M.S. Chen, Y.X. Shen, S.H. Tang, W.S. Shi, D.F. Cui, Z.H. Chen, J. Phys. 12 (2000) 7013–7023.
[32] W.S. Cho, E. Hamada, J. Alloys Compd. 266 (1998) 118–122.
[33] B. Wang, L.D. Zhang, L. Zhang, Y. Yan, S.L. Zhang, Thin Solid Films 354 (1999) 262–266.
[34] A. Scalabrin, A. Chaves, D. Shim, S.P. Porto, Phys. Status Solidi B 79 (1977) 731–742.
[35] R. Naik, J.J. Nazarko, C.S. Flattery, U. Venkateswaran, V. Naik, M.S. Mohammed, G.W. Auner, J.V. Mantese, N.W. Schubring, A.L. Micheli, A.B. Catalan, Phys. Rev. B 61 (2000) 11367–11372.
[36] C. Pithan, Y. Shiratori, R. Waser, J. Dornseiffer, F.H. Haegel, J. Am. Ceram. Soc. 89 (2006) 2908–2916.
[37] R.S. Katiyar, Y.I. Yuzyuk, R.R. Das, P. Bhattacharya, V. Gupta, Ferroelectrics 329 (2005) 907–916.
[38] Y. Liu, K. Zhu, S. Ding, G.G. Siu, in: Proceedings of the XIX International Conference on Raman Spectroscopy ICORS 2004, 8–13 August 2004, Gold Coast, Queensland, Australia, (2004), pp. 516–517.
[39] J.S. Zhu, X.M. Lu, W. Jiang, W. Tian, M. Zhu, M.S. Zhang, X.B. Chen, X. Liu, J. Appl. Phys. 81 (1997) 1392–1395.